EUKARYOTIC CELL, June 2006, p. 954–963 Vol. 5, No. 6
1535-9778/06/$08.00+0 doi:10.1128/EC.00380-05

Nature of the Periplastidial Pathway of Starch Synthesis in the Cryptophyte *Guillardia theta*

Philippe Deschamps,[1] Ilka Haferkamp,[2] David Dauvillée,[1] Sophie Haebel,[3] Martin Steup,[4] Alain Buléon,[5] Jean-Luc Putaux,[6] Christophe Colleoni,[1] Christophe d'Hulst,[1] Charlotte Plancke,[1] Sven Gould,[7] Uwe Maier,[7] H. Ekkehard Neuhaus,[2] and Steven Ball[1]*

CNRS, UMR8576, Cité Scientifique, 59655 Villeneuve d'Ascq, France[1]; Pflanzenphysiologie, Fachbereich Biologie, Technische Universität Kaiserslautern, D-67663 Kaiserslautern, Germany[2]; Center of Mass Spectrometry of Biopolymers[3] and Plant Physiology, Institute of Biochemistry and Biology,[4] University of Potsdam, 14476 Golm, Germany; Institut National de la Recherche Agronomique, Centre de Recherches Agroalimentaires, Rue de la Géraudière, BP 71627, 44316 Nantes Cedex 03, France[5]; Centre de Recherches sur les Macromolécules Végétales, ICMG-CNRS, BP 53, F-38041 Grenoble Cedex 9, France[6]; and Philipps-Universität Marburg, Zellbiologie, Karl von Frisch-Strasse, D-35032 Marburg, Germany[7]

Received 22 December 2005/Accepted 10 March 2006

The nature of the periplastidial pathway of starch biosynthesis was investigated with the model cryptophyte *Guillardia theta*. The storage polysaccharide granules were shown to be composed of both amylose and amylopectin fractions with a chain length distribution and crystalline organization very similar to those of starch from green algae and land plants. Most starch granules displayed a shape consistent with biosynthesis occurring around the pyrenoid through the rhodoplast membranes. A protein with significant similarity to the amylose-synthesizing granule-bound starch synthase 1 from green plants was found as the major polypeptide bound to the polysaccharide matrix. N-terminal sequencing of the mature protein proved that the precursor protein carries a nonfunctional transit peptide in its bipartite topogenic signal sequence which is cleaved without yielding transport of the enzyme across the two inner plastid membranes. The enzyme was shown to display similar affinities for ADP and UDP-glucose, while the V_{max} measured with UDP-glucose was twofold higher. The granule-bound starch synthase from *Guillardia theta* was demonstrated to be responsible for the synthesis of long glucan chains and therefore to be the functional equivalent of the amylose-synthesizing enzyme of green plants. Preliminary characterization of the starch pathway suggests that *Guillardia theta* utilizes a UDP-glucose-based pathway to synthesize starch.

Cryptophytes are composed primarily of photosynthetic, unicellular, biflagellated eukaryotes that are found in a variety of habitats, including oligotrophic freshwater lakes and cold marine environments (for a review, see reference 20). Unlike the case for the glaucophytes or the green and red algae, the plastids of the cryptophytes are surrounded by four membranes. The two innermost membranes define the functional equivalents of the chloroplast, rhodoplast, or cyanelle inner and outer membranes. The third membrane encloses a space known as the periplast, where the nucleomorph and starch granules can be found. The nucleomorph consists of a vestigial eukaryotic nucleus that was recently completely sequenced (15; reviewed in reference 10). This vestigial nucleus bears witness to the endosymbiotic theory and is thought to be the remnant of a red alga nucleus. This red alga was engulfed by a nonphotosynthetic protist, a process known as secondary endosymbiosis. All molecular reports on cryptophytes seem to confirm this hypothesis (10, 15, 16). The outermost membrane of the plastid is thought to be the remnants of the phagocytic vacuole that was later fused to the host endoplasmic reticulum in the stramenopiles (brown algae, diatoms, oomycetes, etc.), haptophytes, and cryptophytes (for a review, see reference 11).

* Corresponding author. Mailing address: CNRS, UMR8576, USTL, Bâtiment C9, Cité Scientifique, 59655 Villeneuve d'Ascq, France. Phone: 33 3 2043 6543. Fax: 33 3 2043 6555. E-mail: steven.ball@univ-lille1.fr.

Secondary endosymbiosis of a red alga gave birth to a series of important eukaryotic lineages that include the chromists, the haptophytes, the alveolates (dinoflagellates, ciliates, and apicomplexan parasites), and the cryptophytes (reviewed in reference 11). Whether one (in the case of the chromalveolate hypothesis) or several distinct secondary endosymbiotic events have yielded this diversity of organisms is still a matter of debate (7, 22). Among the chromalveolates, the dinoflagellates, apicomplexans, and cryptophytes synthesize starch as their storage material, while others store either glycogen (the ciliates) or β-glucans (the stramenopiles and haptophytes).

The cellular localization of the starch in cryptophytes is consistent with the presence of a secondary endosymbiosis event involving a red alga. Indeed, red algae are known to accumulate a form of storage polysaccharide known as floridean starch in their cytoplasm (for reviews of starch metabolism, see references 5 and 33). It was therefore expected to be located in the corresponding periplastidial compartment in cryptophytes. Floridean starches were first thought to display a structure quite different from that of the classical forms of starch accumulating within the plastids of the green algae and land plants (33). Indeed, at first this material was shown to lack amylose, the minor polysaccharide fraction of starch that contains fewer than 1% α-1,6 linkages (for reviews concerning starch structure and amylose synthesis, see references 4 and 8). It was later

found that some unicellular red algae did accumulate amylose within their floridean starch granules (26).

In an effort to understand the process of protein targeting within the different membranes and compartments defined by the secondary plastids, we have cloned a starch synthase cDNA and genomic DNA (19). This gene was chosen in order to study targeting of proteins to the periplastidial space, where starch synthesis is bound to occur. The starch synthase was shown to harbor a N-terminal bipartite topogenic signal, composed of a signal peptide at the N terminus which is then followed by a transit peptide (19). The transit peptide contains a motif different from the nucleus-encoded plastid proteins, thereby trapping it in the periplastidial compartment after transport across the periplastidial membrane.

In this work we report a detailed characterization of the starch structure and metabolic pathway of amylose synthesis in the model cryptophyte *Guillardia theta*. We show that the previously reported starch synthase sequence corresponds to the major granule-bound protein and is the functional homologue of granule-bound starch synthase 1 (GBSS1), which has been proven to be responsible for amylose synthesis in green algae and land plants (4). We also show that the transit peptide is nevertheless cleaved, yielding the mature periplastidial GBSS. Finally, a preliminary study of other components of the starch pathway strongly suggests that cryptophytes use the UDP-glucose pathway of floridean starch biosynthesis. The evolutionary implications of these discoveries are discussed.

MATERIALS AND METHODS

Materials. ADP-[U-^{14}C]glucose, UDP-[U-^{14}C]glucose, α-D-[U-^{14}C]glucose 1-phosphate, and Percoll were purchased from GE Healthcare (formerly Amersham [United Kingdom] and Pharmacia [Sweden]). ADP-glucose, UDP-glucose, ATP, UTP, rabbit liver glycogen, and Sepharose CL-2B were obtained from Sigma-Aldrich (St. Louis, Missouri). Starch assay kits were obtained from Diffchamb (Lyon, France). TSK HW50 and Fractogel TSK DEAE-650 (M) were obtained from Merck (Darmstadt, Germany). Protein assay kits were purchased from Bio-Rad (Munich, Germany).

Algal strains and growth conditions. *Guillardia theta* (strain CCMP327 from the Provasoli-Guillard National Center for Culture of Marine Phytoplankton) was maintained and grown under continuous light (2,000 lx) in h/2 liquid medium (21) with vigorous shaking. Cultures were inoculated at 0.2×10^6 to 0.3×10^6 cells/ml.

Starch preparation. Algal cultures that had just reached stationary phase (around 4 to 5 million cells per ml) were centrifuged ($3000 \times g$, 10 min). The pellets were resuspended and pooled in extraction buffer (20 mM Tris-HCl [pH 7.5], 5 mM EDTA, 1 mM dithiothreitol). The suspension was sonicated, and disrupted cells were centrifuged ($10,000 \times g$, 15 min). Supernatants were kept and used for protein quantification and enzymological studies, while the pellets (starch and cell fragments) were resuspended in 90% Percoll and centrifuged ($10,000 \times g$, 30 min) to separate high-density starch granules from cell debris of lower density. The Percoll gradient step was repeated once to ensure complete removal of cell debris from the starch pellet. The starch was then washed twice in sterile water. Clean white starch pellets were stored at 4°C for up to 1 month.

Determination of starch composition and chain length distribution. Starch or α-1,4 glucan amounts were assayed using the Diffchamb Enzyplus starch kit. The Sepharose CL-2B gel permeation chromatography procedure used is identical to the one we have previously described for *Chlamydomonas* (32). Eluted glucans were detected by measuring the optical density at the maximum absorbance wavelength (λ_{max}) after interaction with iodine. The radioactivity of these fractions was determined by liquid scintillation counting. To determine the chain length distribution, a total of 500 μg of dialyzed and lyophilized amylopectin purified by gel permeation chromatography was suspended in 55 mM sodium acetate (pH 3.5) and debranched with 10 units of *Pseudomonas amylodermosa* isoamylase (Hayashibara Biochemical Laboratory, Okayama, Japan) at 42°C for 12 h. The reaction was stopped by 10 min of boiling, and the sample was subjected to high-performance anion-exchange chromatography with pulsed amperometric detection (HPAEC-PAD) as described for *Chlamydomonas* (17).

X-ray diffraction, differential scanning calorimetry (DSC), and scanning electron microscopy (SEM). X-ray diffraction was performed after adjustment of the water content by water desorption at 90% relative humidity for 10 days under partial vacuum in the presence of a saturated barium chloride solution. The sample (10 mg) was then sealed between two tape foils to prevent any significant change in water content during the measurement. The diffraction diagram was recorded using an Inel (Artenay, France) spectrometer at 40 kV and 30 mA in the Debye-Scherrer transmission mode. The X-ray radiation Cukα1 (λ = 0,15405 nm) was selected with a quartz monochromator. Diffraction diagrams were recorded during 2-h exposure periods with a curve position sensitive detector (Inel CPS 120). Relative crystallinity was determined after normalization of all recorded diagrams at the same integrated scattering between 2θ values of 3° and 30°. Spherulitic A-type recrystallized amylose was used as a crystalline standard after scaled subtraction of an experimental amorphous curve in order to obtain null intensity in the regions without diffraction peaks. Dry extruded potato starch was used as the amorphous standard. The degree of crystallinity of structures resulting from α(1,4) chain precipitation was determined using the method initially developed by Wakelin et al. (35) for cellulose.

For DSC, samples (about 20 mg) were weighed in stainless steel high-pressure pans, and about 80 μl of distilled water was added before sealing. An automated heat flux differential scanning calorimeter (SETARAM DSC 121) was used, and scans between 20 and 180°C were run at 3°C/min and ±40 mW full scale. Calibration was checked using indium (429.6 K) and gallium (302.7 K) melting. The reference cell contained 100 μl water. Melting enthalpies were calculated with respect to dry matter, after water content determination using sequential drying at 50°C overnight and at 130°C for 6 h. For SEM, drops of aqueous suspensions of purified starch granules were deposited onto copper stubs and allowed to dry. The specimens were coated with Au-Pd and observed in secondary electron imaging mode with a JEOL6100 microscope.

Extraction of granule-bound starch proteins, SDS-PAGE, and Western blotting. Western blot analyses were performed to estimate the amounts of GBSS1 and ADP-glucose pyrophosphorylase small subunit. GBSS1 protein was extracted by denaturing 50 μg of starch granules in 80 μl of denaturating solution (2% sodium dodecyl sulfate [SDS] and 5% β-mercaptoethanol) for 10 min. The samples were centrifuged for 20 min at $10,000 \times g$, and then supernatants were loaded onto a 7.5% SDS-polyacrylamide gel. For ADP-glucose pyrophosphorylase, the equivalent of 20 μg of total protein was separated by 10% SDS-polyacrylamide gel electrophoresis (SDS-PAGE). Proteins were separated by SDS-PAGE according established procedures (23). After migration, both polyacrylamide gels were electroblotted onto polyvinylidene difluoride membranes (Hybond-P; Amersham Biosciences) in transfer buffer (48 mM Tris, 39 mM glycine, 0.0375% [wt/vol] SDS, and 20% methanol) for 2 h at room temperature and 100 mA, using the Mini Trans-Blot Cell (Bio-Rad, Hercules). The blots were washed twice for 10 min in TBS buffer (10 mM Tris-HCl [pH 7.5], 150 mM NaCl) and then blocked for 1 hour in TBS containing 5% skim milk. The blocking buffer was removed, and membranes were further washed twice for 10 min each in T-TBS buffer (20 mM Tris-HCl, 500 mM NaCl, 0.05% Tween 20) and incubated with primary antibody. The Western blot analysis with the antibody raised against the GBSS1 protein was as previously described (36). The anti-ADP-glucose pyrophosphorylase (anti-AGPase) antibody was a kind gift from Curtis Hannah (University of Florida, Gainesville). This polyclonal antibody, directed against the maize endosperm small subunit (bt2) of the enzyme (18), was diluted 1:5,000 in blocking buffer, and blots were incubated overnight at 4°C. This antibody displays a strong cross-reaction against the proteins from *Escherichia coli*, cyanobacteria, *Ostreococcus taurii*, and *Chlamydomonas reinhardtii*. Membranes were washed twice for 10 min each in T-TBS buffer and incubated with a 1:10,000 dilution of donkey anti-rabbit secondary antibody conjugated with horseradish peroxidase (Amersham Biosciences). The antigen-antibody complex was visualized by chemiluminescence (Amersham Biosciences).

GBSS enzyme assay. Purified starch granules (500 μg) were incubated at 30°C in 100 μl of 50 mM Tris-HCl (pH 7.5), 0.47% mercaptoethanol, 5.5 mM $MgCl_2$, 3.2 mM sugar-nucleotide (ADP-Glc or UDP-Glc), and 2.2 μM of the respective ^{14}C-radiolabeled sugar-nucleotide at 304 mCi/mmol. Tubes were shaken at 1,400 rpm during incubation, and the reaction was stopped by adding 900 μl 70% ethanol. The granules were washed twice with 1 ml 70% ethanol and resuspended in 200 μl water. The label incorporated was measured by liquid scintillation counting.

In vitro synthesis of amylose. Two milligrams of purified starch granules was incubated in the same buffer as described above, except the concentrations of sugar-nucleotides (labeled and unlabeled) were both doubled. For analysis of starch after in vitro synthesis of amylose, granules were washed and resuspended

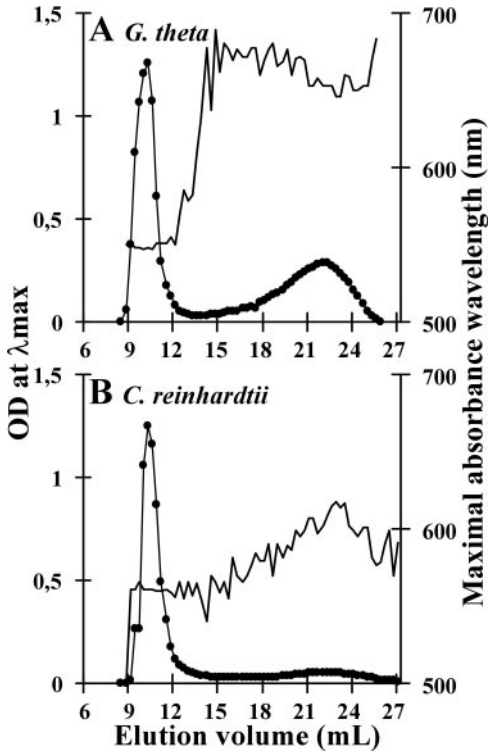

FIG. 1. Separation of amylopectin and amylose by size exclusion chromatography. Two milligrams of starch purified from nitrogen-supplied cultures grown under constant illumination of *Guillardia theta* (A) and *Chlamydomonas reinhardtii* (B) were subjected to Sepharose CL-2B chromatography. For each fraction, the optical density (OD) (●) of the iodine-polysaccharide complex was measured at the λ_{max} (—). Due to its very high molecular weight, the amylopectin is excluded as a single sharp peak from the Sepharose column. This peak displays a red iodine stain with a λ_{max} at 540 nm. The second peak displays the population of amylose molecules with a typical green color (λ_{max} above 600 nm). The difference in color is due to the differences in iodine-polysaccharide interaction quality generated by the presence of significantly longer chains in amylose.

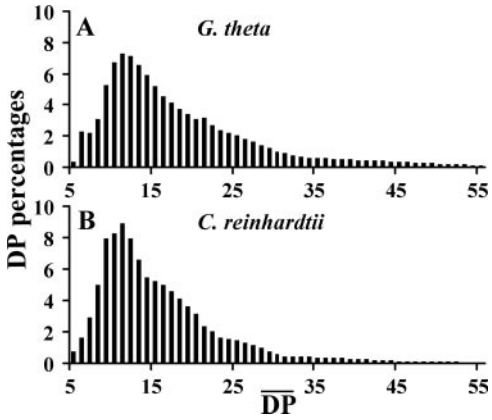

FIG. 2. Chain length distribution of isoamylase-debranched amylopectin. Five hundred micrograms of amylopectin obtained from CL-2B chromatography of *Guillardia* (A) and *Chlamydomonas* (B) was debranched using isoamylase, and the linear glucans were subjected to HPAEC-PAD. The *x* axis shows the degree of polymerization ($\overline{DP}$) of the glucans, while *y* axis shows the percentage of each type of glucan.

in 200 μl of 90% dimethyl sulfoxide (DMSO) and boiled at 100°C for 10 minutes. Solubilized glucans were precipitated with 800 μl ethanol at −20°C for at least 2 h. After centrifugation, the glucan pellet was resuspended in 10 mM NaOH and subjected to CL-2B chromatography.

Analysis of debranched glucans from starch subjected to in vitro synthesis of amylose. Two milligrams of starch was subjected to in vitro synthesis of amylose, dissolved in 90% DMSO, and precipitated with ethanol as described above. Two milligrams of nonradiolabeled starch was prepared by an identical procedure. The two preparations were mixed together, and after centrifugation, the starch pellet was subjected to isoamylase debranching (see above). The reaction was stopped by boiling, the DMSO concentration was raised to 10% to avoid retrogradation of long glucans, and the sample was immediately subjected to TSK-HW50 gel permeation chromatography (32). Eluted glucans were detected by iodine staining, and each fraction was assayed for radioactivity by scintillation counting.

ADP-glucose and UDP-glucose pyrophosphorylase assay. ADP-Glc and UDP-Glc pyrophosphorylases were assayed in the direction of sugar-nucleotide synthesis as follows. Twenty-five micrograms of crude extract protein was incubated for 15 min at 30°C in 75 mM HEPES/KOH (pH 7.5), 0.5 mM ATP or UTP, 3.5 mM $MnCl_2$, 25 μg/ml bovine serum albumin, 0.4 mM Glc-1P, and 2.6 μM α-D-[U-^{14}C]glucose 1-phosphate (150 mCi/mmol), and the reaction was stopped by heating at 100°C for 10 min. Unincorporated Glc-1P was removed by a 2-hour incubation at 30°C with 3 units of calf intestine alkaline phosphatase (Roche, Mannheim, Germany) to avoid unspecific radioactive contamination of the filters with labeled Glc-1P during the next step. Samples were filtered and washed with water (six times, 10 ml) on DE81 anion-exchange filters (Whatman, Maidstone, United Kingdom). The filters were dried, and radioactivity was measured by scintillation counting.

Zymogram analysis of starch synthase activities and starch-metabolizing enzymes. Two hundred micrograms of crude extract proteins was loaded on a 35:1 (acrylamide:bisacrylamide), 7.5% (1.5-mm-thick) polyacrylamide gel containing 0.3% rabbit liver glycogen and run under native conditions. Electrophoresis was carried out at 4°C at 15 V cm^{-1} for 180 min, using the Mini-Protean II cell (Bio-Rad) in 25 mM Tris-glycine (pH 8.3) and 1 mM dithiothreitol. After migration, the gel was incubated overnight in 50 mM Tris-HCl (pH 7.5), 100 mM $(NH_4)_2SO_4$, 20 mM β-mercaptoethanol, 5 mM MgCl2, 0.5 mg/ml bovine serum albumin, and 1.2 mM ADP-Glc or UDP-Glc at 25°C. The reaction was stopped, and the gel was stained by adding an iodine solution (0.25% KI and 0.025% I_2). For detection of starch-metabolizing enzymes, the same procedure was followed except that glycogen was replaced by 0.3% potato starch (Sigma) and gels were incubated after migration in 25 mM Tris-glycine (pH 8.3) and 5 mM EDTA.

Partial purification of starch synthase activities from crude extract. The procedure for partial purification of starch synthase activities from crude extract is derived from the protocol published for purification of *Gracilaria tenuistipitata* UDP-Glc-utilizing soluble starch synthase (28). For this purpose, crude extracts were prepared as described above except that 0.5 mM benzamidine and 1 mM phenylmethylsulfonyl fluoride were added to the extraction buffer, and the extract was filtered on a 0.45-μm-pore-size filter. All steps were performed at 4°C. Proteins were incubated in the presence of glycogen (2.5% final concentration) for 30 min, precipitated by raising the polyethylene glycol 8000 concentration to 7.5%, and centrifuged at 3,000 × *g* for 20 min. The supernatant was discarded and the glycogen pellet resuspended in 15 ml of extraction buffer. The glycogen-mediated precipitation was repeated once, and the pellet was resuspended in 5 ml extraction buffer and loaded on a Fractogel TSK DEAE-650 (M) anion-exchange column (20-cm length, 2-cm inner diameter) equilibrated with extraction buffer. The column was washed with the same buffer until no glycogen was detected in the eluant. Activities were eluted in a two-step procedure, first with 0.1 M KCl and then with 0.3 M KCl. Pooled proteins from these elutions, from the flowthrough, and from the different supernatants were assayed for starch synthase activity by a radioactivity assay (28) and with zymograms. Together, these data show that starch synthases are eluted from the anion-exchange column during the first elution, while the bulk of starch-catabolizing activities are retained in the column until the second elution. The same radioactivity assay was then used for partial characterization of the starch synthase activities.

RESULTS

Morphology and structure of *Guillardia theta* starch granules. Two previous studies on the nature of the storage polysaccharides accumulated by *Chilomonas paramecium* (2) and *Chroomonas salina* (1) established that cryptophytes accumu-

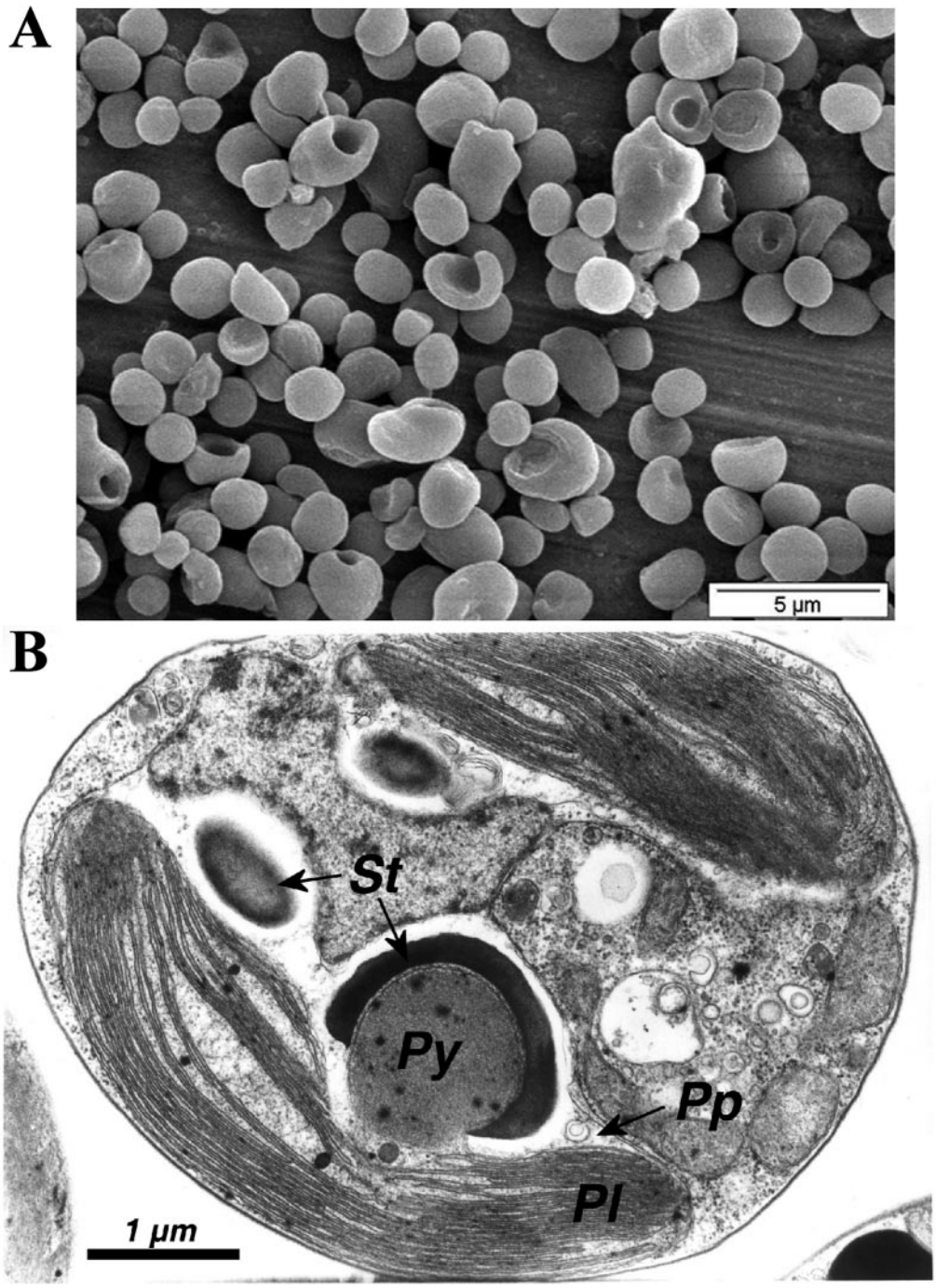

FIG. 3. Panel A. Scanning electron microscopy of native purified starch granules from *Guillardia theta*. Many granules display an unusual round cavity, probably due to a close association with the pyrenoid during their synthesis. Panel B. Transmission electron microscopy of a cross section of *Guillardia theta* treated with brefeldin A. The plastid (Pl) contains a single pyrenoid (Py) and is surrounded by the periplast (Pp). A starch granule (St) is growing around the pyrenoid, separated from this latter by the inner double membrane of the plastid. Other starch granules can be seen in the periplast.

lated α-1,4-linked and α-1,6-branched glucans in a 15:1 to 32:1 proportion. In addition, the polysaccharide was reported to be stained with iodine with a λ_{max} of the iodine polysaccharide complex of 605 nm (1). According to those authors, these results are consistent with the presence of amylose-containing starch granules broadly ressembling potato starch. In order to get a more detailed picture of the storage polysaccharides, we separated the low-molecular-weight amylose from amylopectin by gel permeation chromatography (Fig. 1). The amylose and amylopectin fractions were separately pooled. Amylopectin was then subjected to enzymatic debranching through treatment with isoamylase followed by HPAEC-PAD (Fig. 2) anal-

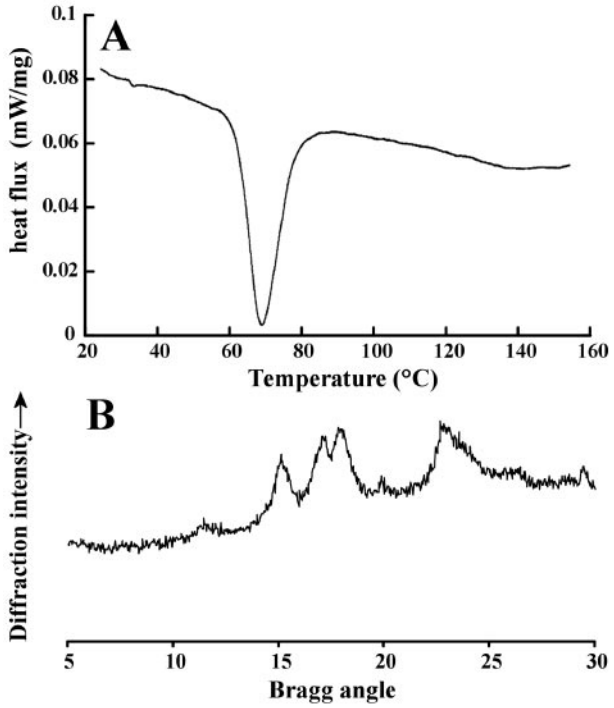

FIG. 4. Physicochemical analysis of starch extracted from *Guillardia theta*. Panel A. DSC thermogram. The major endotherm is attributed to the melting of the hydrogen-bonded double-helical structures (starch gelatinization). The thermogram, which can be compared to those previously reported for *Chlamydomonas* (9), characterizes starches with normal levels of crystallinity (around 30%). Panel B. Wide-angle X-ray diffractogram. Diffraction peaks at 2θ (Bragg angle) values of 9.9°, 11.2°, 15°, 17°, 18.1°, and 23.3° characterize an A-type starch like the one found in *Chlamydomonas* (9).

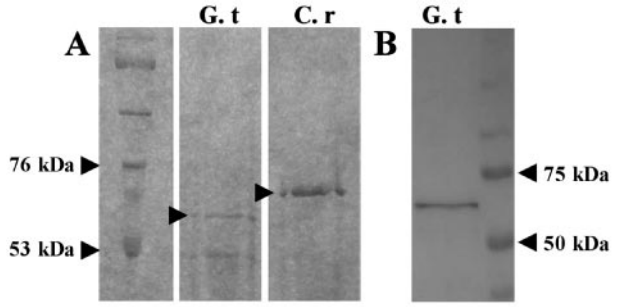

FIG. 5. Visualization of the starch granule-bound proteins. Panel A. Coomassie blue stain after SDS-PAGE of total protein extracted by boiling with SDS (see Materials and Methods) from 2 mg of purified starch granules. G. t and C. r, *Guillardia theta* and *Chlamydomonas reinhardtii*, respectively. The major starch-bound protein of *Guillardia* shows an apparent molecular mass of about 60 kDa, which is a standard size for a plant GBSS1. GBSS1 from *Chlamydomonas* is known to have a 10-kDa C-terminal extension that gives it an apparent molecular mass closer to 70 kDa. Panel B. Western blot analysis of granule-bound proteins extracted from 50 μg of starch of *Guillardia theta*. The antibody used in this experiment was designed to react against a peptide that defines a highly conserved C-terminal region of plant GBSS proteins (36). Molecular mass marker references are indicated. Note that panels A and B display different gels that contained different sets of molecular mass markers. The masses were calculated from the position of each set of markers.

ysis. This analysis enables the separation of the polysaccharide unit chains according to their degree of polymerization. Chains differing in size by only one glucose residue can be neatly separated and quantified by such techniques, thereby yielding a detailed chain length distribution for the debranched polysaccharide. The results displayed in Fig. 2 establish that the chain length distribution of the periplastidial starch of *Guillardia theta* closely resembles that reported for the green alga *Chlamydomonas reinhardtii* or the unicellular red alga *Rhodella violacea* (29) and differs significantly from the structures reported for potato tuber starch. In particular, the mass distribution of the amylose molecules displayed in Fig. 1 is similar to those of *Chlamydomonas* and cereal endosperm starch (25).

Starch differs from glycogen by its insoluble nature. The starch polymers (amylopectin and amylose) aggregate into huge insoluble granules whose number, shape, and size are genetically controlled. We thus investigated the morphology of such granules by electron microscopy. As seen in Fig. 3A, when observed by SEM, most granules display an ovoid shape with a size ranging from 1 to 3 μm. A few larger granules (3 to 5 μm) with a more elongated shape are also seen. However, a significant number of granules display a highly unusual ball-shaped cavity. By analogy with *Chlamydomonas reinhardtii* starch accumulation, we infer that these cavities result from localized polysaccharide synthesis around the pyrenoid, a proteinaceous body composed essentially of ribulose-1,5-bisphosphate carboxylase/oxygenase (Rubisco). Examination of cross sections of *Guillardia theta* by transmission electron microscopy confirmed these speculations (Fig. 3B). Indeed, some starch granules clearly associate with the intraplastidial pyrenoid on the periplastidial face of the plastid's second (outer) membrane.

Amylopectin is responsible for building the backbone of starch granules. Neighboring chains within clusters intertwine into parallel double helices that assemble into highly specific crystalline lattices (reviewed in reference 8). The lattices diffract and give two types of X-ray diffraction patterns corresponding to two different assembly geometries that have been named A type and B type. Starch is typically semicrystalline, as only sections of amylopectin assemble into crystals, while amylose is usually a mostly amorphous fraction. The *Guillardia theta* starch granules were thus further analyzed using X-ray diffraction. The results shown in Fig. 4A establish that *Guillardia theta* synthesizes semicrystalline starch polymers of the A type, with a crystallinity of about 32%. The assembly of amylopectin into double-helical semicrystalline structures can also be investigated through measurement of the energy required to melt such structures. This and other issues that result from the semicrystalline nature of the polymers can be addressed by differential scanning calorimetry. As shown in Fig. 4B, a melting temperature of 70°C and an enthalpy of 12.9 J/g were determined by DSC. These values are in agreement with those published for many common starches, including that of *Chlamydomonas* (9). Together with the results displayed in Fig. 1, 2, and 4, these data demonstrate that cryptophytes accumulate starch with a structure very similar to that of the starch from vascular plants and green algae.

Identification of the major granule-bound protein as the previously identified starch synthase gene. In *Chlamydomonas reinhardtii* and land plants, amylose is synthesized through the

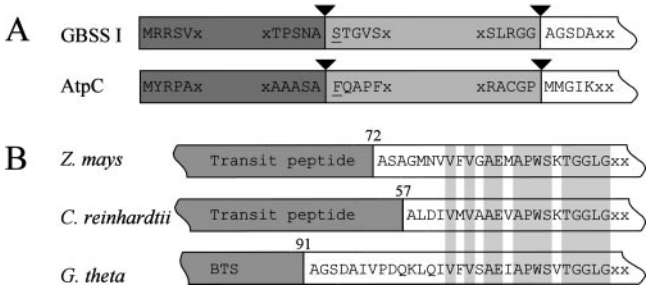

FIG. 6. Panel A. The bipartite topogenic signal of the periplastidial GBBSI is displayed in comparison with that of the plastidial *G. theta* AtpC (ATPase gamma subunit). Nucleus-encoded proteins that function either in the periplastidial compartment or in the plastid display the same basic features. A signal peptide (dark gray) drives the preprotein cotranslationally into the endoplasmic reticulum lumen, where it is cleaved off. The second part is in both cases predicted to be a transit peptide (light gray), which serves for translocation into the periplastidial compartment (GBSS1) or the plastid (AtpC) by an unknown mechanism. The triggering difference resides in the phenylalanine that is present in all plastid proteins at the +1 position of the transit peptide (underlined). The GBSS1 shows a serine at this position. Panel B. Schematic comparison of the cleavage sites leading to mature GBSS proteins of *Zea mays*, *Chlamydomonas reinhardtii*, and *Guillardia theta*. N-terminally cleaved peptides are either transit peptides (corn and *Chlamydomonas*) or a bipartite topogenic signal (Guillardia). The vertical light gray bars show the homologies between the three mature protein sequences. Numbers indicate the amino acid positions of the cleavage sites within each sequence. This alignment shows that the beginnings of the mature GBSS proteins are well conserved among species, even if the targeting peptides are functionally different and therefore nonhomologous.

action of granule-bound starch synthase from ADP-glucose. The presence of a classical amylose fraction in *Guillardia theta* starch prompted us to look for an analogous enzyme bound to the polysaccharide matrix. Proteins eluted by boiling of starch granules with SDS are displayed in Fig. 5A. The major protein bound to starch was investigated by trypsin digestion and mass spectroscopy analysis of the fragmented peptides. The peptide sequences and mass spectrometric analysis matched perfectly the sequence of the *Guillardia theta* starch synthase that we had previously cloned (19). N-terminal sequencing of the putative GBSS1 protein was achieved. This sequence (AGSDAI VPD) established that the bipartite topogenic signal including the transit peptide-like sequences was successfully cleaved off the mature protein at a position significantly downstream from that predicted had the transit peptide been classically functional. The nature and position of the residues responsible for targeting the GBSS1 within the periplastidial space are detailed in Fig. 6.

Kinetic properties of the *Guillardia theta* GBSS1. The *Guillardia* GBSS activity was characterized with respect to its apparent affinity towards ADP-glucose and UDP-glucose and its optimal temperature (55°C) and pH (6.5). The apparent K_ms for UDP-glucose and ADP-glucose were found to be similar (3.8 ± 0.3 mM and 2.7 ± 0.1 mM, respectively), while the V_{max} was only twofold higher when UDP-glucose (32 ± 5 nmol · h^{-1} · mg^{-1}) rather than ADP-glucose (17 ± 3 nmol · h^{-1} · mg^{-1}) was used. Because maltooligosaccharides are known to activate the plant GBSS1 (14, 32), we examined the impact of maltotriose (50 mM) with respect to the enzyme activity (Fig. 7A). The enzyme was activated 15-fold in the presence of 50 mM

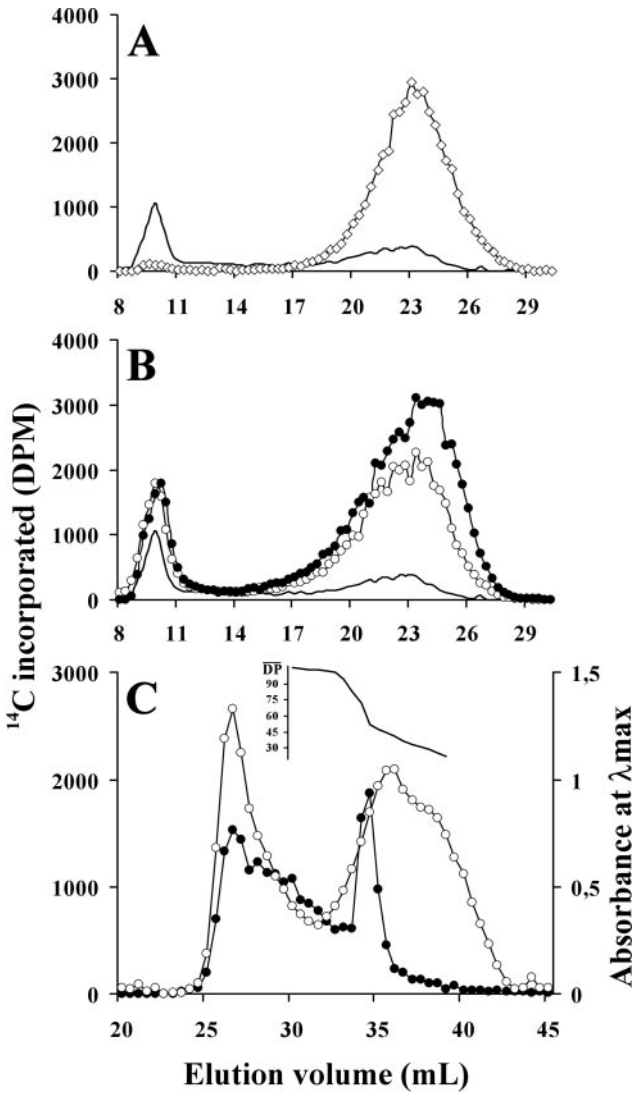

FIG. 7. Analysis of in vitro synthesis of amylose. Native purified starch granules of *Guillardia theta* were subjected to in vitro synthesis in the presence of ^{14}C-labeled UDP-Glc. After the reaction, amylopectin and amylose were separated by CL-2B Sepharose chromatography, and scintillation counting of radioactivity was performed for each fraction. Panel A. Effect of maltooligosaccharides on the reaction observed after 1 hour of in vitro synthesis. When maltotriose is added (◇) the incorporation of labeled glucose is highly enhanced compared to the normal rate (—) and is found predominantly in the amylose fraction. This behavior is typical of a GBSS activity. Panel B. Analysis of in vitro synthesis without maltooligosaccharides after 1 h (—), 4 h (○) and 12 h (●). Note that the bulk of the amylose is synthesized later than that of the amylopectin. Panel C. Separation of isoamylase-debranched glucans from total starch by TSK HW-50 chromatography. Two milligrams of native starch granules was mixed with 2 mg of starch subjected to 12 h of in vitro synthesis of amylose in the presence of ^{14}C-labeled UDP-Glc. After debranching of the total starch with isoamylase, glucans were separated by TSK HW-50 size exclusion chromatography. Eluted glucans were detected through their iodine-polysaccharide interaction. The optical density (○) of the complexes was measured at λ_{max}. The incorporation of ^{14}C was also assayed in each fraction (●). The curve in the top part of the panel shows the average degree of polymerization ($\overline{DP}$) of the glucans in the fractions, calculated as described by Banks et al. (6). ^{14}C was incorporated only into long chains in both amylose and amylopectin. This behavior is typical of a "GBSS-like" activity, while soluble starch synthases are not able to produce glucans with an average $\overline{DP}$ higher than 50 under such experimental conditions.

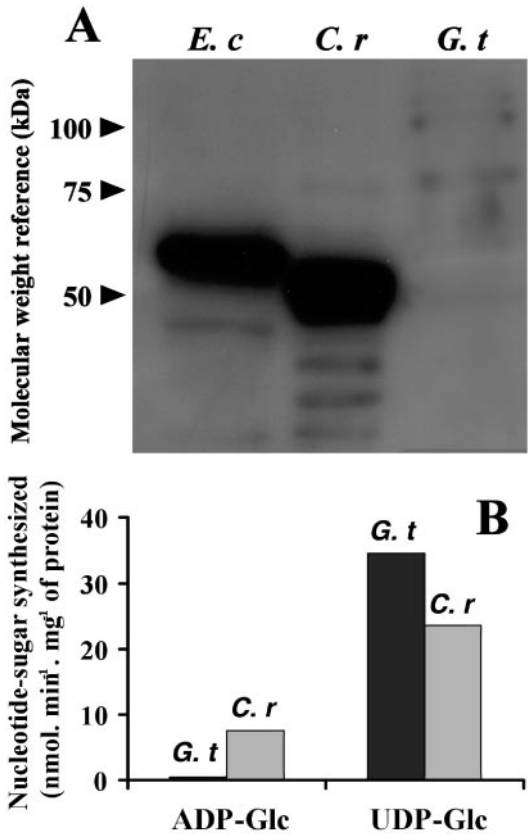

FIG. 8. Probing for the presence of ADP-Glc pyrophosphorylase in *Guillardia theta*. Panel A. Western blot analysis of soluble proteins from *E. coli* (E. c), *Chlamydomonas reinhardtii* (C. r), and *Guillardia theta* (G. t), using an antibody raised against the small subunit of maize ADP-Glc pyrophosphorylase (see Materials and Methods). This antibody shows a strong enough cross-reaction with such a wide variety of species (from bacteria to vascular plants) that the absence of a corresponding ADP-Glc pyrophosphorylase protein in *Guillardia theta* can be considered significant. Panel B. ADP-Glc and UDP-Glc pyrophosphorylase assays performed in the direction of synthesis. ATP or UTP was provided to 25 μg of soluble proteins together with α-D-[U-^{14}C]glucose 1-phosphate. *Chlamydomonas reinhardtii* crude extracts were used as an ADP-Glc pyrophosphorylase positive control for comparison with the same amounts of *Guillardia theta* extracts.

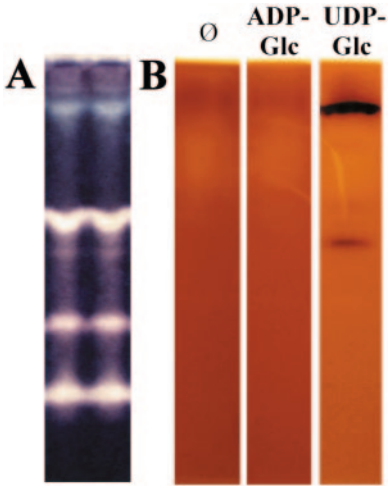

FIG. 9. Detection of starch-metabolizing enzymes by zymograms. Native gel electrophoresis with either starch (A) or glycogen (B) was performed with 100 μg of protein per lane and a crude extract of *Guillardia theta*. Gels containing glycogen were incubated with ADP-Glc, UDP-Glc, or neither of the two (Ø). Brown bands due to glucosylnucleotide-dependent glucosyl transfer reactions were observed only when UDP-Glc was used. At least four activities active on starch were detected. By comparison with other organisms, the upper blue bands are suggestive of the presence of an isoamylase activity. The pink-white bands could correspond to either branching enzyme or amylase activities.

maltotriose, and the label was essentially incorporated in the amylose fraction. In the absence of the maltooligosaccharide the label was found predominantly on amylopectin during short incubation times, while after 4 h the label was found predominantly on amylose (Fig. 7B). Whether found in amylopectin or amylose, the label was always found to be incorporated in the long-chain fraction upon debranching of the polysaccharide product (Fig. 7C). This situation is identical to the one we previously reported for the *Chlamydomonas* GBSS1, where through pulse-chase experiments we were able to prove that the chains were first extended on amylopectin and then cleaved off into the amylose fraction (32). However the low specific activity of the *Guillardia* GBSS1, which is over 40-fold lower than that of *Chlamydomonas* GBSS1, and the fact that the starting material was already filled with amylose thwarted all attempts to reproduce such chase experiments with the cryptophyte GBSS1. Nevertheless, the properties listed above for the *Guillardia* GBSS1 unambiguously identify it as the major amylose-synthesizing enzyme.

***Guillardia* contains at least one UDP-glucose-utilizing soluble starch synthase and no detectable ADP-glucose-synthesizing or -utilizing enzymes.** The biochemical properties of *Guillardia theta* GBSS1 show only a very modest preference towards UDP-glucose compared to ADP-glucose. In order to find out if *Guillardia* utilizes the green plant (ADP-glucose-based) or, more logically, the red alga (UDP-glucose-based) pathway of starch synthesis, we investigated the presence of AGPase, the enzyme responsible for ADP-glucose synthesis. We performed Western blotting (Fig. 8A) and enzyme assays (Fig. 8B), which failed to detect traces of AGPase. The polyclonal antibody (a kind gift from Curtis Hannah) used was produced against the maize small subunit and displayed strong cross-reactions against a wide variety of species. Zymogram gels (Fig. 9) clearly showed the presence of the classical enzymes of starch metabolism together with a UDP-glucose-utilizing soluble starch synthase activity. This enzyme activity was purified 20-fold through its affinity for glycogen. The ratio of activities measured with the semipure enzyme in the presence of UDP-glucose versus ADP-glucose ranged between 6 and 10 when measured at 0.2 to 10 mM glycosylnucleotide, respectively. This marked preference for UDP-glucose explains the specificity of the activity revealed on our zymogram gels.

DISCUSSION

This study reports on the first characterization of GBSS1 in the red alga lineage. This enzyme was discovered and intensively studied in the green lineage as the major determinant of amylose synthesis, the unbranched fraction of starch. GBSS1 is

an enzyme that requires binding to a semicrystalline granule to be normally active, and its presence correlates with that of amylose-containing starches (4). Red algae were first thought to accumulate starch devoid of amylose in the cytoplasm. The presence of amylose was, however, relatively recently reported for a number of unicellular red algae, including *Rhodella violacea* (26). Older reports characterizing the structure of starch in cryptophytes and dinoflagellates clearly mention the presence of amylose in these polysaccharides (1, 2, 34). Since these pioneering studies, it has been proposed that these organisms were derived from one (12) or several (7) secondary endosymbiotic events involving a red algal symbiont and a flagellated heterotrophic eukaryotic host. It thus seems logical to suppose that the red alga symbiont(s) contained both amylose and GBSS1.

We have previously proposed that the pathway of starch synthesis in both red and green algae resulted from the merging of a preexisting pathway of glycogen synthesis from the host and that of storage polysaccharide from the cyanobacterial symbiont after primary endosymbiosis (13). Recent evidence points to the existence of starch-like polymers in some cyanobacteria (27), but amylose-containing true starch granules remain to be described for present-day cyanobacteria. Nevertheless, phylogenetic trees such as those displayed in Fig. 10 clearly relate green alga and *Guillardia* GBSS1 sequences to cyanobacterial glycogen synthases and particularly to those of *Crocosphaera watsoni*, a unicellular diazotrophic cyanobacterium. We therefore infer that during primary endosymbiosis of the plastid, the GBSS1 gene from the cyanobacterial symbiont was transferred to the nucleus of the host and retained in the red alga lineage together with those enzymes of bacterial origin that are known to be involved in the biogenesis of semicrystalline polysaccharide, as previously suggested (13).

This gene was subsequently lost in all chromists, together with all other enzymes of the starch pathway. Alveolates, on the other hand, have maintained the pathway of starch synthesis. Apicomplexans have probably simplified their genomes according to their parasitic lifestyle (13). The genes that were lost include all "redundant" functions such as GBSS1, whose activity is not mandatory to obtain normal levels of storage polysaccharide granules. Ciliates such as *Tetrahymena* or *Paramecium*, on the other hand, have selectively lost isoamylase, an enzyme that we have previously demonstrated to be required to obtain semicrystalline polysaccharides, and have therefore reverted to glycogen synthesis. They have also lost those enzymes directly interacting with the semicrystalline starch granules (such as GBSS1 and the glucan water dikinase, an enzyme required for starch degradation). We presently have no real clues as to why the cryptophytes have maintained a pathway of starch synthesis in the periplast. Evidently, as stressed in this work, *Guillardia theta* has maintained a privileged association of starch metabolism with the pyrenoid. Pyrenoids of green and red algae have been proven to be composed of an organized proteinaceous assembly of Rubisco and other Calvin cycle enzymes (reviewed in reference 3). This assembly divides at the time of plastid division to generate in most cases a single pyrenoid per plastid. In chlorophytes the pyrenoid is suspected to define a major component of the carbon concentration mechanism in a fashion analogous but not identical to that for the cyanobacterial carboxysome (which, in addition to Rubisco, contains carbonic anhydrase). In green algae the pyrenoid is surrounded by a starch sheath which is not in itself required for operation of the carbon concentration mechanism (3).

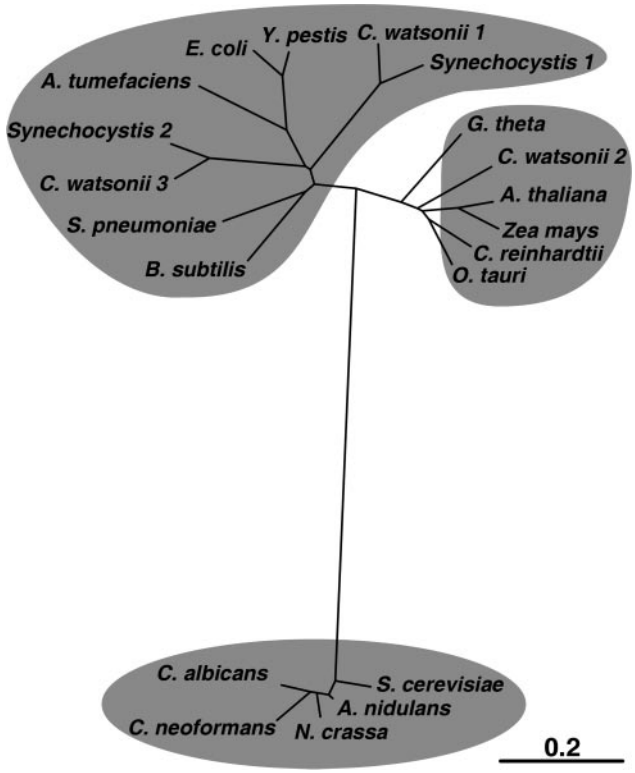

FIG. 10. Phylogenetic tree of glycogen and starch synthases. The protein sequence of the presently studied "GBSS-like" enzyme (accession no. AJ784213) was compared with sequences of four class of enzymes: "yeast like" glycogen synthases of *Neurospora crassa* (AAC98780), *Aspergillus nidulans* (EAA58813), *Candida albicans* (EAK99020), *Cryptococcus neoformans* (AAW45795), and *Saccharomyces cerevisiae* (AA88715); bacterial glycogen synthases of *E. coli* (AAC76454), *Bacillus subtilis* (CAB15073), *Yersinia pestis* (AAM87434), *Streptococcus pneumoniae* (AAK99836), and *Agrobacterium tumefaciens* (AAL44876); cyanobacterial glycogen synthases of *Synechocystis* sp. strain PCC6803 isoform 1 (BAA18625) and isoform 2 (BAA16625) and three isoforms of *Crocosphaera watsonii* (EAM53362, EAM48230, and EAM48998); and plant GBSS1 from *Arabidopsis thaliana* (AAF31273), *Chlamydomonas reinhardtii* (AAL28128), *Ostreococcus tauri* (AAS88890), and *Zea mays* (AAQ06291). Sequences were aligned by using ClustalW (31), and the sequence alignment was manually improved by using BioEdit (T. Hall). The unrooted phylogenetic tree was build using neighbor joining. The scale bar represents the number of substitutions per site. All node bootstrap values except the *Saccharomyces cerevisiae* node (at 56) were above 80. This tree shows that the protein of *Guillardia theta* is closely related to the family of plant GBSS1 proteins.

In some "primitive" unicellular red algae (the Porphyridiales), such as the unicellular amylose-containing *Rhodella violacea*, the association with the intraplastidial pyrenoid is not lost despite the presence of starch in the cytoplasm (24). In this case, the starch associates with the pyrenoid, which is surrounded and separated from the polysaccharide by the inner and outer membranes of the rhodoplast (24). As this work suggests, such an association seems to have been maintained in cryptophytes and may define one of the factors for conservation of periplastidial starch synthesis. Localized synthesis of

starch across membranes has important implications with respect to our understanding of starch biosynthesis and particularly with respect to granule morphogenesis. Indeed, it is evident from this work and observations made with many green algal species that the pyrenoid dictates the shape of a significant proportion of starch granules. The shape of the pyrenoidal starch can be easily explained if synthesis occurs predominantly at the polysaccharide-pyrenoid interface. This interface is obviously defined by the rhodoplast membranes in the cases of *Guillardia* and unicellular red algae. In the case of green algae, the pyrenoid is also thought to be separated from the starch sheath by a membrane. As hypothesized by Süss et al. (30) following their immunogold localization of Calvin cycle enzymes, multienzyme complexes may be localized at the stromal surface of this membrane. It is tempting to speculate that starch metabolism enzymes may colocalize with these complexes.

The biochemical characterization of the GBSS1 enzyme reported here clearly shows that the cryptophyte enzyme displays properties very similar if not identical to those of similar enzymes of the green lineage. An important distinction between the *Guillardia* and plant enzymes can be found in the glycosylnucleotide substrate preferences. While the plant GBSS1 displays a marked preference for the ADP-glucose substrate, the *Guillardia* enzyme displays only a twofold-higher V_{max} when using UDP-glucose than when using ADP-glucose. In addition, both substrates are used with similar apparent affinities. These results, while consistent with the presence of the UDP-glucose-based pathway of the red lineage that we recently suggested (13), do not make a very convincing case for it. For this reason, we have demonstrated that ADP-glucose pyrophosphorylase activity is absent in these organisms and have characterized a partly purified soluble starch synthase activity. This enzyme displayed a marked preference for UDP-glucose. We therefore propose that cryptophytes such as the red algae utilize a UDP-glucose-based pathway of starch synthesis.

ACKNOWLEDGMENTS

This research was funded by the French Ministry of Education and the Centre National de la Recherche Scientifique (CNRS) (support to S.B. and J.L.P.), l'Institut National de la Recherche Agronomique (support to A.B.), the Deutsche Forschungs Gemeinschaft (grants SFB 593 [support to U.M.] and SFB 429 [support to M.S]), and the Deutsche Forschungs Gemeinschaft Schwerpunkt Intrazelluläres Leben (support to H.E.N.).

We are grateful to B. Pontoire and J. Davy (INRA, Nantes, France) for the X-ray diffraction and differential scanning calorimetry measurements, respectively.

REFERENCES

1. **Antia, N. J., J. Y. Cheng, R. A. J. Foyle, and E. Percival.** 1979. Marine cryptomonad starch from autolysis of glycerol-grown *Chroomonas salina*. J. Phycol. **15:**57–62.
2. **Archibald, A. R., E. L. Hirst, D. J. Manners, and J. F. Riley.** 1960. Studies on the metabolism of protozoa. VIII. The molecular structure of a starch-type polysaccharide from *Chilomonas paramecium.* J. Chem. Soc. **1960:**556–560.
3. **Badger, M. R., T. J. Andrews, S. M. Whitney, M. Ludwig, D. C. Yellowlees, W. Leggat, and G. D. Price.** 1998. The diversity and coevolution of Rubisco, plastids, pyrenoids, and chloroplast-based CO_2-concentrating mechanisms in algae. Can. J. Bot. **76:**1052–1071.
4. **Ball, S., M. van de Wal, and R. Visser.** 1998. Progress in understanding the biosynthesis of amylose. Trends Plant Sci. **3:**462–467.
5. **Ball, S. G., and M. K. Morell.** 2003. Starch biosynthesis. Annu. Rev. Plant Biol. **54:**207–233.
6. **Banks, W., C. T. Greenwood, and K. M. Khan.** 1971. The interaction of linear amylose oligomers with iodine. Carbohydr. Res. **17:**25–33.
7. **Bodyl, A.** 2005. Do plastid-related characters support the chromalveolate hypothesis? J. Phycol. **41:**712–719.
8. **Buléon, A., P. Colonna, V. Planchot, and S. Ball.** 1998. Starch granules: structure and biosynthesis. Int. J. Biol. Macromol. **23:**85–112.
9. **Buléon, A., D.-J. Gallant, B. Bouchet, G. Mouille, C. D'Hulst, J. Kossman, and S. G. Ball.** 1997. Starches from A to C. Chlamydomonas reinhardtii as a model microbial system to investigate the biosynthesis of the plant amylopectin crystal. Plant Physiol. **115:**949–957.
10. **Cavalier-Smith, T.** 2002. Nucleomorphs: enslaved algal nuclei. Curr. Opin. Microbiol. **5:**612–619.
11. **Cavalier-Smith, T.** 2003. Genomic reduction and evolution of novel genetic membranes and protein targeting machinery in eukaryote-eukaryote chimaeras (meta-algae). Philos. Trans. R. Soc. London B **359:**109–134.
12. **Cavalier-Smith, T.** 1998. A revised six-kingdom system of life. Biol. Rev. Camb. Philos. Soc. **73:**203–226.
13. **Coppin, A., J. S. Varre, L. Lienard, D. Dauvillee, Y. Guerardel, M. O. Soyer-Gobillard, A. Buleon, S. Ball, and S. Tomavo.** 2005. Evolution of plant-like crystalline storage polysaccharide in the protozoan parasite *Toxoplasma gondii* argues for a red alga ancestry. J. Mol. Evol. **60:**257–267.
14. **Denyer, K., B. Clarke, C. Hylton, H. Tatge, and A. Smith.** 1996. The elongation of amylose and amylopectin chains in isolated starch granules. Plant J. **10:**1135–1143.
15. **Douglas, S. E., S. Zauner, M. Fraunholz, M. Beaton, S. Penny, L. T. Deng, X. Wu, M. Reith, T. Cavalier-Smith, and U. G. Maier.** 2001. The highly reduced genome of an enslaved algal nucleus. Nature **410:**1091–1096.
16. **Douglas, S. E., and S. L. Penny.** 1999. The plastid genome of the cryptophyte alga, Guillardia theta: complete sequence and conserved synteny groups confirm its common ancestry with red algae. J. Mol. Evol. **48:**236–244.
17. **Fontaine, T., C. D'Hulst, M. L. Maddelein, F. Routier, T. M. Pepin, A. Decq, J. M. Wieruszeski, B. Delrue, N. Van den Koornhuyse, J. P. Bossu, B. Fournet, and S. Ball.** 1993. Toward an understanding of the biogenesis of the starch granule. Evidence that Chlamydomonas soluble starch synthase II controls the synthesis of intermediate size glucans of amylopectin. J. Biol. Chem. **268:**16223–16330.
18. **Giroux, M. J., and L. C. Hannah.** 1994. ADP-glucose pyrophosphorylase in *shrunken2* and *brittle2* mutants of maize. Mol. Gen. Genet. **243:**400–408.
19. **Gould, S. V., M. S. Sommer, K. Hadfi, S. Zauner, P. G. Kroth, and U. G. Maier.** Protein targeting into the complex plastid of cryptophytes. J. Mol. Evol., in press.
20. **Graham, L. E., and L. W. Wilcox.** 2000. Algae, p. 169–179. Prentice-Hall, Upper Saddle River, N.J.
21. **Guillard, R. R. L.** 1975. Culture of phytoplankton for feeding marine invertebrates, p. 26–60. *In* W. L. Smith and M. H. Chanley (ed.), Culture of marine invertebrate animals. Plenum Press, New York, N.Y.
22. **Harper, J. T., E. Waanders, and P. J. Keeling.** 2005. On the monophyly of chromalveolates using a six-protein phylogeny of eukaryotes. Int. J. Syst. Evol. Microbiol. **55:**487–496.
23. **Laemmli, U. K.** 1970. Cleavage of structural proteins during the assembly of the head of bacteriophage T4. Nature **227:**680–685.
24. **Lee, R. E.** 1974. Chloroplast structure and starch grain production as phylogenetic indicators in the lower rhodophyceae. Br. Phycol. J. **9:**291–295.
25. **Libessart, N., M. L. Maddelein, N. Van Den Koornhuyse, A. Decq, B. Delrue, G. Mouille, C. D'Hulst, and S. G. Ball.** 1995. Storage, photosynthesis and growth: the conditional nature of mutations affecting starch synthesis and structure in *Chlamydomonas reinhardtii*. Plant Cell **7:**1117–1127.
26. **McCracken, D. A., and J. R. Cain.** 1981. Amylose in floridean starch. New Phytol. **88:**67–71.
27. **Nakamura, Y., J. I. Takahashi, A. Sakurai, Y. Inaba, E. Suzuki, S. Nihei, S. Fujiwara, M. Tsuzuki, H. Miyashita, H. Ikemoto, M. Kawachi, H. Sekiguchi, and N. Kurano.** 2005. Some cyanobacteria synthesize semi-amylopectin type α-polyglucans instead of glycogen. Plant Cell Physiol. **46:**539–545.
28. **Nyvall, P., J. Pelloux, H. V. Davies, M. Pedersen, and R. Viola.** 1999. Purification and characterisation of a novel starch synthase selective for uridine 5′-diphosphate glucose from the red alga *Gracilaria tenuistipitata*. Planta **209:**143–152.
29. **Rahaoui, A.** 1999. Ecophysiologie de *Rhodella violacea* (rhodophyta): production et propriétés structurales des exopolysaccharides et de l'amidon floridéen. Ph.D. thesis. Université des Sciences et Technologies de Lille, Villeneuve d'Ascq, France.
30. **Süss, K. H., I. Prokhorenko, and K. Adler.** 1995. *In situ* association of Calvin cycle enzymes, ribulose-1,5-*bis*phosphate carboxylase/oxygenase activase, ferredoxine-NADP reductase, and nitrite reductase with thylakoid and pyrenoid membranes of *Chlamydomonas reinhardtii* chloroplasts as revealed by immunoelectron microscopy. Plant Physiol. **107:**1387–1397.
31. **Thompson, J. D., D. G. Higgins, and T. J. Gibson.** 1994. ClustalW: improving the sensitivity of progressive multiple sequence alignment through sequence weighting, position-specific gap penalties and weight matrix choice. Nucleic Acids Res. **22:**4673–4680.
32. **van de Wal, M., C. D'Hulst, J. P. Vincken, A. Buléon, R. Visser, and S. Ball.** 1998. Amylose is synthesized *in vitro* by extension of and cleavage from amylopectin. J. Biol. Chem. **273:**22232–22240.

33. **Viola, R., P. Nyvall, and M. Pedersen.** 2001. The unique features of starch metabolism in red algae. Proc. R. Soc. London B **268:**1417–1422.
34. **Vogel, K., and B. J. D. Meeuse.** 1968. Characterization of the reserve granules from the dinoflagellate *Thecadinium inclinatum* Balech. J. Phycol. **4:**317–318.
35. **Wakelin, J. H., H. S. Virgin, and E. Crystal.** 1959. Development and comparison of two X-ray methods for determining the crystallinity of cotton cellulose. J. Appl. Physiol. **30:**1654–1662.
36. **Wattebled, F., A. Buleon, B. Bouchet, J. P. Ral, L. Lienard, D. Delvalle, K. Binderup, D. Dauvillee, S. Ball, and C. D'Hulst.** 2002. Granule-bound starch synthase. I. A major enzyme involved in the biogenesis of B-crystallites in starch granules. Eur. J. Biochem. **269:**3810–3820.